J Nanopart Res (2013) 15:1791
DOI 10.1007/s11051-013-1791-2

RESEARCH PAPER

Controlled self-decoration of $Mo_6S_yI_z$ ($8.2 \leq y + z \leq 10$) nanowires and their transformation to MoS_2 nanotubes with gold nanoparticles

Andrej Kovič · Damjan Vengust · Mojca Vilfan · Aleš Mrzel

Received: 7 February 2013 / Accepted: 11 June 2013

Abstract Nanowires and nanotubes decorated with gold nanoparticles are known for their excellent sensing and catalytic properties. However, the decoration of transition–metal dichalcogenide nanotubes can be very complex. Here we report on a simple procedure that enables efficient production and purification of thin bundles of $Mo_6S_yI_z$ ($8.2 \leq y + z \leq 10$) nanowires decorated with gold nanoparticles and their transformation to gold-decorated MoS_2 nanotubes. We isolated several hundred milligrams of nanowire bundles that were several microns long with average diameters of around 40 nm, and formed a stable dispersion in water without added surfactants. Gold nanoparticles were directly deposited on the nanowire bundles either in a solution or on a substrate at room temperature in a single-step reaction without any additional reducing reagents. The number of gold nanoparticles on a nanowire bundle is controlled by changing the concentration of chloroauric acid $HAuCl_4 \cdot 3H_2O$ in the solution. Since the nanowires can serve as precursor crystals for fabrication of nanotubes, we were able to transform gold-decorated nanowires and produce gold-decorated MoS_2 nanotubes.

Keywords Nanowires · Nanotubes · Self-decoration · Gold nanoparticles

A. Kovič · D. Vengust · M. Vilfan (✉) · A. Mrzel
J. Stefan Institute, Jamova 39, 1000 Ljubljana, Slovenia
e-mail: mojca.vilfan@ijs.si

Introduction

Inorganic nanowires, nanotubes, nanorods, and nanobelts have recently attracted considerable attention mainly due to their electronic and optoelectronic properties that make them suitable for applications in nanodevices and nanosensors (Burda et al. 2005; Hernández-Vélez 2006; Yogeswaran and Chen 2008; Ramgir et al. 2010). Because of their very high surface-to-volume ratios, these quasi-one-dimensional materials are much more sensitive to external influences than similar two-dimensional thin films. A slight change in coating significantly changes their electrical properties, enabling detection of single molecules (Wanekaya et al. 2006; Lee et al. 2012). Another very promising possibility of using inorganic nanowires as sensors is by decorating them with gold nanoparticles (Joshi et al. 2009; Singh et al. 2011; Syed and Bokhari 2011). Gold nanoparticles are a very frequent and important tool in nanotechnology, mainly due to their chemical stability, bio-compatibility, their easy surface functionalization or bio-conjugation, and surface-plasmon resonance (Daniel and Astruc 2004; Xia and Halas 2005; Homola 2008). Besides, they easily form Au–S bonds with molecules that contain thiol group (–SH). Gold-decorated nanowires are thus very suitable for a broad set of different applications, including molecular recognition and biomolecular sensing (Syed and Bokhari 2011).

It has been shown previously that $Mo_6S_yI_z$ ($8.2 \leq y + z \leq 10$) nanowires have unique optical

Published online: 21 June 2013

and electronic properties (Gadermaier et al. 2007; Vrbanič et al. 2007) and can act as precursor material for bulk production of several types of molybdenum-based nanowires and nanotubes (Remškar et al. 2009; Domenici et al. 2011). Standard procedure for the production of $Mo_6S_yI_z$ ($8.2 \leq y + z \leq 10$) nanowires is a single-step process: elements are heated to above 1,000 °C in an evacuated quartz ampoule (Vrbanič et al. 2004). The product materials have a diameter of several hundred nanometers and the vast majority of the material is not dispersible in polar solvents. Synthetic methods using a two-zone furnace with a temperature gradient enable production of thinner and shorter bundles (Remškar et al. 2011). In this case, the material is produced directly from the elements at a molar ratio Mo:S:I of 6:3:9. However, the obtained bundles with the diameters of around 100 nm and lengths up to 10 μm are still poorly dispersible in water. Another method (Kovič et al. 2012) enables synthesis of yet thinner bundles that grow in a hedgehog-like morphology. In this case, the starting materials were previously synthesized bundles of nanowires with larger diameters. Both methods yield materials that contain large amounts of impurities and a procedure for isolation of thinner bundles and thus production of pure material has not yet been presented.

It has been shown previously that sulfur atoms at the ends of nanowires can form covalent bonds with a gold surface or with thiol groups of large biomolecules (Ploscaru et al. 2007). However, the method in which the nanowires are just mixed with the solution of prepared gold nanoparticles turned out not to be very effective as only a small fraction of nanowires had gold particles attached, either to the ends or to the surface (Compagnini et al. 2010). A simpler and slightly more efficient method is based on adding different amounts of $HAuCl_4$ to the dispersion of nanowires in boiling water in the presence of a reducing agent (Zhang et al. 2010).

Here we report on a different procedure for production and isolation of thin bundles of $Mo_6S_yI_z$ ($8.2 \leq y + z \leq 10$) nanowires and on their very efficient decoration with gold nanoparticles. The goal of the synthesis is to produce thin nanowires, soluble in water without added surfactants. Good solubility is required for uniform distribution of gold nanoparticles on the nanowire surface. Decoration with gold is done in a single step at room temperature without reducing agents, and results in decoration of both side walls and ends of bundles. Using water solution of $HAuCl_4$ as a source of gold, the bundles can be self-decorated either in water dispersion or when previously deposited on a substrate. Number of gold nanoparticles on nanowires is controlled simply by changing the concentration of $HAuCl_4$.

The obtained nanowires can be further sulfurized to gold-decorated MoS_2 nanotubes. This is especially important as the layered transition-metal dichalcogenide nanotubes often show high inertness to chemical and biological functionalization, limiting their potential for applications (Tahir et al. 2006). As the $Mo_6S_yI_z$ ($8.2 \leq y + z \leq 10$) nanowires serve as precursors for other types of molybdenum-based nanomaterials, we can implement the same procedure for obtaining a variety of other gold-decorated molybdenum-based nanowires and nanotubes.

Experimental and characterization

Sample preparation

Bundles of $Mo_6S_yI_z$ ($8.2 \leq y + z \leq 10$) nanowires were synthesized directly from the elements in a one-step procedure. In a typical experiment, 1,500 mg of molybdenum (Aldrich, 99.98 %), 417 mg of sulfur (Aldrich, 99.98 %) and 661 mg of iodine (Aldrich, 99.999 %), all in powder form, were sealed in a quartz ampoule and placed in a two-zone furnace. The ampoule was left for three days in a temperature gradient with lower temperature being 750 °C and higher temperature 850 °C. At lower temperature end of the 25-cm long ampoule, a free-standing foil composed of vertically aligned nanowires was obtained (up to 10 wt%). At the higher temperature end, the remaining material was a dark-brown powder. We have shown previously that the obtained powder consists of bundles of nanowires, molybdenum grains and MoS_2 crystals (Rangus et al. 2008). The collected powder was washed several times with ethanol to remove weakly bound iodine. Dried material was then put in acetonitrile and sonicated in a low-power ultrasonic bath (40 W, 40 kHz) for 15 min, yielding a stable dispersion of the material. After sonication, the supernatant was extracted and separated by centrifugation (1,030×g for 15 min) to remove heavier MoS_2 crystals and molybdenum grains. The remaining material was microfiltrated and dried at 50 °C, with

resulting yield around 10–15 wt%. From this material, which was completely dispersible in acetonitrile, isolation of thinner bundles was performed by further centrifugation: first at 3,500×*g* to remove any remaining heavier aggregates and larger bundles; then the supernatant was extracted and centrifuged at 8,000×*g* for 10 min. The supernatant from the second step contained smaller impurities, mostly parts of broken nanowire bundles and MoS_2 flakes. The remaining sediment was re-dispersed in acetonitrile using mild ultrasonic agitation for 10 min. The final concentration of nanowire bundles in acetonitrile was estimated to be up to 70 mg/l. The acetonitrile dispersion was finally microfiltrated and the material was dried at 50 °C.

The first step toward a successful decoration of nanowire bundles with gold was to verify if the nanowires had enough redox potential for reducing $[AuCl_4]^-$ in aqueous solution without added reducing agents. We put 50 mg of unpurified nanowire powder obtained directly from the synthesis into 20 ml of 2.5 mM solution of $HAuCl_4$ (Aldrich, $HAuCl_4{\cdot}3H_2O$) in ultra-pure water (18.2 MΩ-cm, Millipore purification system) for 1 h. The solution of $HAuCl_4$ was initially light yellow with pH of about 5.0. After adding the nanowire powder, the yellow solution became more transparent and the color of the powder changed from dark brown to reddish brown within a few minutes. This clearly indicated reduction of chloroauric acid and suggested successful decoration.

For decoration of purified nanowire bundles, around 20 mg of $Mo_6S_yI_z$ ($8.2 \leq y + z \leq 10$) were first dispersed in 1,000 ml of ultra-pure water and ultrasonicated for 30 min. Later 10 ml of $HAuCl_4$ solution in water were added to the dispersion under ultrasonic agitation and the reaction took place during 45 min. Two different concentrations of $HAuCl_4$ in water were used (0.25 and 2.5 mM) to study the influence of concentration on the number and size of gold nanoparticles deposited on the nanowire surface. The resulted $Mo_6S_yI_z$ ($8.2 \leq y + z \leq 10$)/Au composites were collected by centrifugation at 3,460×*g*, rinsed three times with ultra-pure water and dried at 50 °C. The obtained material was easily re-dispersed in water, ethanol or acetonitrile.

To coat the nanowires with gold nanoparticles not in a solution but deposited on a substrate, two sets of samples were prepared. The first set was made by spraying the stable suspension of nanowires in acetonitrile with an airbrush onto a silicon wafer (N-type ⟨100⟩, 2.5 cm × 2.5 cm), which was previously washed with acetone and ethanol. By adjusting the spraying parameters, such as the nozzle size, air flow rate, dispersion concentration, and the distance between nozzle and substrate, quite uniformly deposited nanowire bundles were obtained with little agglomeration. The evaporation of the solvent during the spraying process was accelerated by heating the substrate with a back-heating source to approximately 60 °C. The silicon substrate with deposited nanowires was then dipped into the solution of $HAuCl_4$ in water without stirring. After 45 min, the sample was carefully removed from the solution, rinsed several times with ultra-pure water and dried at 50 °C.

The second set of samples was prepared by applying diluted dispersion of purified nanowires in acetonitrile directly onto a Formvar/carbon coated copper grid (400 mesh, Electron Microscopy Sciences). Excess dispersion was removed with a filter paper and the sample was left to dry. The grids with deposited nanowire bundles were then immersed into 0.0025 and 0.025 mM solutions of $HAuCl_4$. These concentrations of chloroauric acid were the same as when preparing the first set of samples. After 1 h, the grids were taken out of the solution, careful rinsed with ultra-pure water and dried at 50 °C.

Transformation of decorated $Mo_6S_yI_z$ ($8.2 \leq y + z \leq 10$) nanowires to MoS_2 nanotubes was done with sulfurization at 800 °C in flowing Ar gas containing 2 % of H_2S and 1 % of H_2 as described previously (Remškar et al. 2009). The transformation reaction time was 1 h.

For cyclic voltammetry measurements, stable round nanowire films with a diameter of around 5 mm were prepared from 70 ml of stable dispersion of nanowires in acetonitrile (40 mg/l) by passing a microfiltration system. The sample was prepared by fixing the film onto the working electrode of a ceramic patterned electrode (Au, Pine Research Instrumentation) with 3 μl of conductive gold paste. The working electrode with the attached film was insulated at the sides with Torr Seal epoxy resin.

Characterization

The materials were observed and analyzed by scanning electron microscope (SEM, Jeol JSM-7600F) equipped with energy-dispersive spectrometer (EDS),

and high-resolution transmission electron microscope (HR-TEM, Jeol JEM-2100F, 200 keV) with selected area electron diffraction (SAED). TEM grids were prepared from nanowire dispersions immediately after sonication by applying 30 μl of diluted dispersion (5 % mixture in isopropanol) to a Formvar/carbon coated copper grid. The diameters of nanowires, nanotubes and gold nanoparticles were determined using Image Pro Analyzer. Distributions in particle size were obtained by evaluating at least 100 nanoparticles per sample.

Samples were also characterized by X-ray powder diffraction (XRD) at room temperature using a Bruker AXS D4 Endeavor diffractometer with Cu-Kα1 radiation and Sol-X energy-dispersive detector within the angular range 2θ from 10° to 70° with a step size of 0.02° and a collection time of 2 s at a rotation of 6 rpm. In addition, a HP 8453 UV–Vis spectrophotometer was used to collect data from samples, dispersed in water. The absorption spectra were recorded for wavelengths from 200 to 1,000 nm (±1 nm).

Cyclic voltammetry was performed by a Metrohm Autolab PGSTAT302N high current potentiostat/galvanostat using tetrabutylammonium perchlorate (0.1 M) in acetonitrile as the electrolyte. The cyclic voltammograms of the films were obtained from single-piece complete three-electrode cells with a sweep rate of 100 mV/s in the range $-2\ \text{V} < U < 1\ \text{V}$. The cycle and experiments were repeated several times (>20) to ensure the stability of the electrode and reproducibility of the result.

Results and Discussion

$Mo_6S_yI_z$ ($8.2 \leq y + z \leq 10$) nanowires

Dark-brown powder that remained at the hot zone of the chemical transport reaction is shown in Fig. 1a. The SEM image shows bundles of nanowires that grow on unreacted molybdenum grains. The majority of the bundles are self-organized in a hedgehog-like shape. To confirm the composition of this material, X-ray diffraction was performed and the obtained pattern is presented in Fig. 1b. The XRD spectrum clearly shows the presence of unreacted molybdenum, however, also distinct peaks that can be contributed to $Mo_6S_yI_z$ ($8.2 \leq y + z \leq 10$) nanowires and MoS_2 are visible.

By changing the molar ratio of sulfur and iodine in the initial mixture, we were able to synthesize bundles with different diameters. Since our goal was to synthesize nanowire bundles as thin as possible to achieve a stable water dispersion and increase the surface-to-volume ratio, we tried several different ratios of reaction parameters. We discovered that the diameters of bundles strongly depended on the ratio between molybdenum, sulfur, and iodine in the starting mixture, and that the yield of the transported material depended on the reaction time. Seven different molar ratios were tested at a couple of different reaction times. While some mixtures did not produce nanowires at all (the ones with less sulfur and more iodine), we obtained the largest mass yield of the

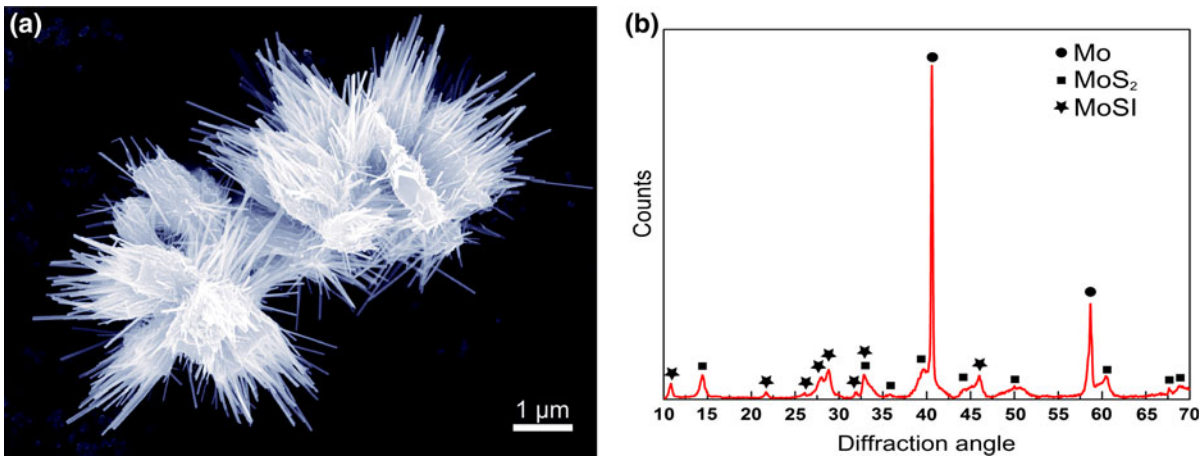

Fig. 1 SEM image of the synthesized material obtained directly from the chemical transport reaction (**a**). XRD of the same material (**b**) showing its composition: $Mo_6S_yI_z$ ($8.2 \leq y + z \leq 10$) nanowires (*asterisks*), MoS_2 (*squares*), and Mo (*circles*)

bundles in the material at a molar ratio molybdenum:sulfur:iodine of 6:5:2 at a reaction time of 72 h. However, the average diameter of these bundles was rather large, about 150 nm. By keeping the molar ratio of the starting mixture and reducing the reaction time to 60 h, we were able to obtain thinner bundles. Although the thickest ones still had a diameter of up to 100 nm, the majority of the bundles was around 60–70 nm thick at a length of up to 5 μm. At these reaction conditions, around 95 wt% of the total synthesized material remained at the hot end of the ampoule.

The experiments described above were all made with 150 μm molybdenum powder. However, we find that the grain size of the powder influences the diameters of the synthesized nanowire bundles. Using 1–2 μm molybdenum powder (Sigma-Aldrich, molybdenum powder 1–2 μm, 99.9 %) at the same conditions, we were able to achieve bundles with typical diameter of 40–50 nm. In addition, yield of the synthesized $Mo_6S_yI_z$ $(8.2 \leq y + z \leq 10)$ bundles grown on the surface of smaller molybdenum grains almost doubled to about 20 %.

After the synthesis and after each step of the purification procedure, SEM was carried out to investigate the composition of the sample. The material obtained after the first microfiltration is shown in Fig. 2a and the corresponding XRD image in Fig. 2c. The SEM image shows large nanowire bundles with impurities that can be identified by XRD

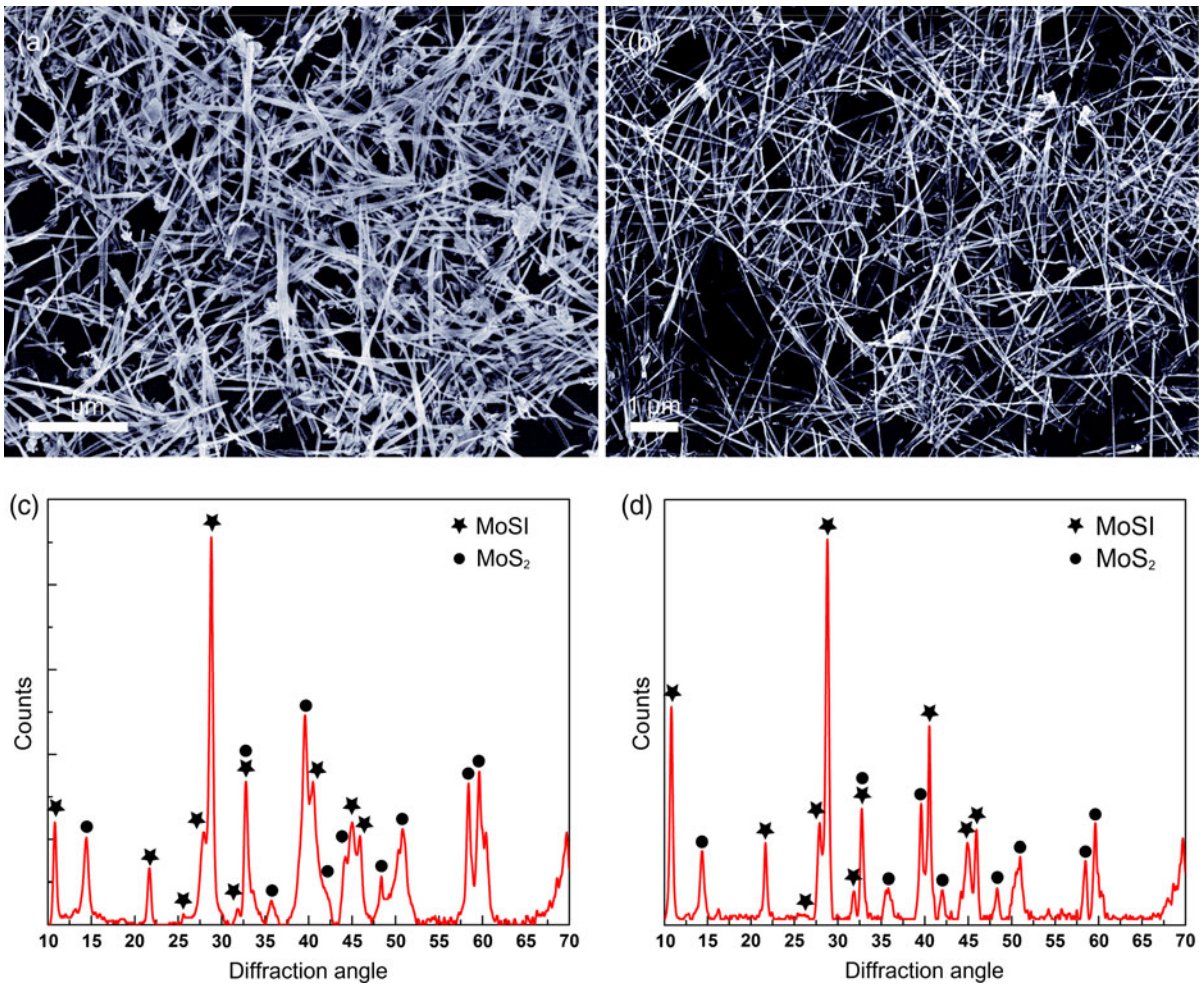

Fig. 2 SEM images of $Mo_6S_yI_z$ $(8.2 \leq y + z \leq 10)$ nanowire bundles after the first (**a**) and after the final microfiltration (**b**). Corresponding XRD spectra are presented in (**c**, **d**). Both spectra show the presence of MoS_2; however, the amount of MoS_2 after the final microfiltration is reduced

as MoS_2. Following the centrifugation at 3,500×g, during which the larger bundles and heavier impurities sedimented, there was another centrifugation at 8,000×g. The sediment after the second centrifugation contained thin $Mo_6S_yI_z$ ($8.2 \leq y + z \leq 10$) bundles with smaller diameters and significantly fewer impurities (Fig. 2b). However, the XRD pattern of the purified nanowires (Fig. 2d) still shows the presence of MoS_2. These XRD patterns show an excellent agreement with previously published XRD spectra of $Mo_6S_3I_6$ (Vrbanič et al. 2004) and $Mo_6S_4I_6$ (Remškar et al. 2011). This further confirms the idea that nanowires of different stoichiometry grow in skeletal structures composed of one-dimensional polymer chains of Mo_6–chalcogen–halogen clusters, which differ only in the site occupied by sulfur and iodine (Meden et al. 2005).

Morphology of one of the thinner synthesized nanowires as seen with high-resolution TEM is presented in Fig. 3a: well crystallized with a high aspect ratio, grown in a longitudinal direction along the [001] axis. Surface of the nanowire is relatively clean without any significant depositions of amorphous coating. Selected area diffraction pattern (SAED) obtained on a single nanowire (Fig. 3b) shows consistency with previously published data obtained on bulk material by X-ray diffraction (Vrbanič et al. 2004; Meden et al. 2005). Their data were used to draw the circles that coincide with the observed pattern.

Decoration of nanowires with gold nanoparticles

Our goal was to decorate $Mo_6S_yI_z$ ($8.2 \leq y + z \leq 10$) nanowires with gold nanoparticles. The result of the initial experiment, which was carried out to verify the possibility of decoration in water at room temperature without a reducing agent, is shown in Fig. 4a. One clearly sees the nanowire hedgehog densely covered with gold nanoparticles, leading to the conclusion that the method was successful. We find that gold nanoparticles appear on nanowires already after a couple of minutes, whereas a prolonged (overnight) deposition results in whole nanowires covered with gold.

A proof that the observed material are indeed $Mo_6S_yI_z$ ($8.2 \leq y + z \leq 10$) nanowires covered with gold is given by the energy-dispersive X-ray spectrum (EDS), shown in Fig. 4b.

Decoration of purified nanowires was done by stepwise introducing $HAuCl_4$ to the dispersion. Mixtures were prepared by adding up to five times 10 ml of 0.25 mM solution and up to three times 10 ml of 2.5 mM $HAuCl_4$ in water to 1,000 ml of the dispersed nanowires (20 mg/1,000 ml). Formation of gold nanoparticles occurred at room temperature and was visible as changes in the color from yellow to

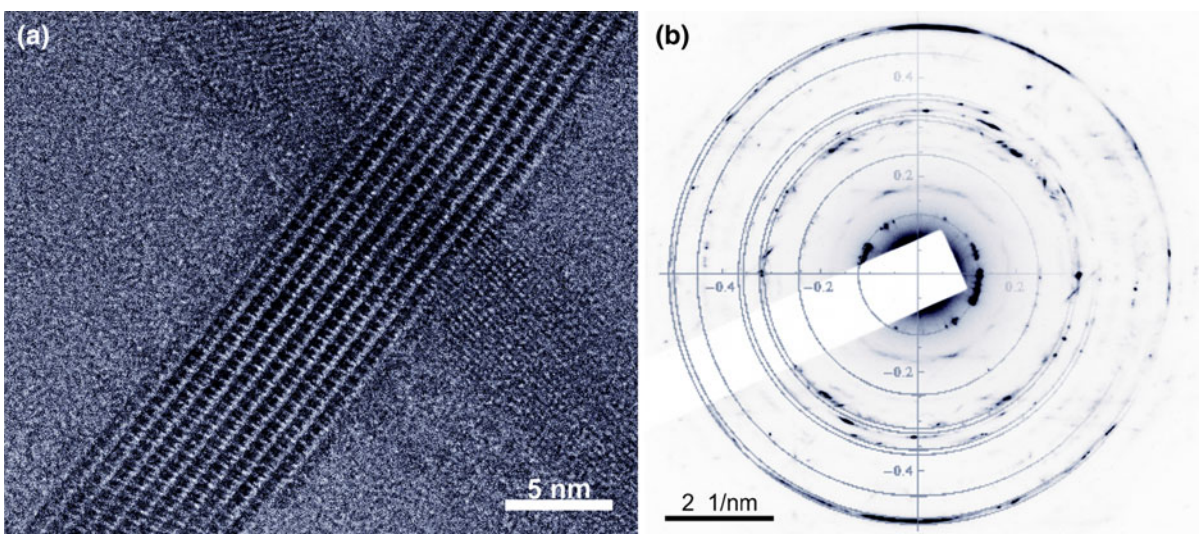

Fig. 3 TEM image of a $Mo_6S_yI_z$ ($8.2 \leq y + z \leq 10$) nanowire bundle (**a**) and SAED pattern (**b**). The bundle shown is one of the thinner ones with the diameter of around 8 nm. The diffraction pattern is consistent with previously published data obtained by bulk X-ray diffraction (Vrbanič et al. 2004; Meden et al. 2005), depicted as *gray circles*. For clarity, the *circles fade out* so that the observed pattern is visible

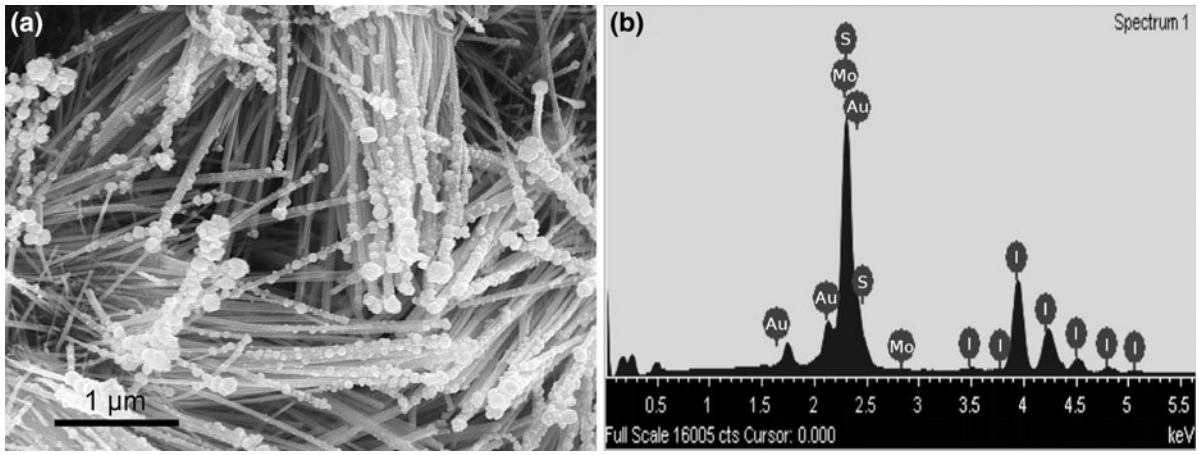

Fig. 4 SEM image of $Mo_6S_yI_z$ ($8.2 \leq y + z \leq 10$) nanowire hedgehog covered with gold nanoparticles (**a**) and EDS spectrum confirming the composition of the obtained material (**b**)

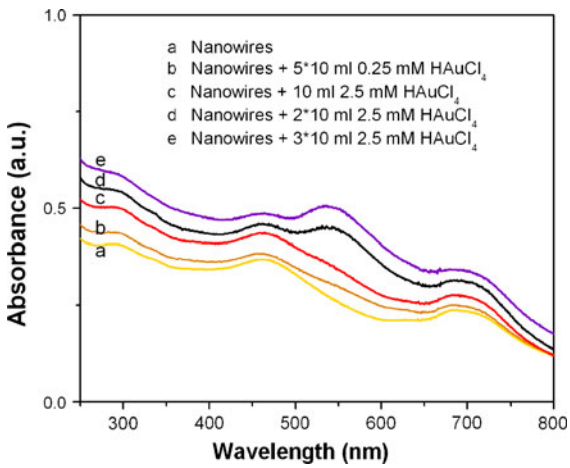

Fig. 5 UV–Vis spectra of dispersions of gold-decorated nanowires. Three peaks are visible on pure nanowires (**a**), but when increasing the amount of the added chloroauric acid, a prominent peak emerges at around 540 nm that corresponds to gold nanoparticles (**b–e**)

brown-yellow when adding lower-concentration solution, and yellow to violet-red when adding higher concentration solution of gold complex. Such color transitions are characteristic for changes that occur in the oxidation state of gold ions and the formation of gold nanoparticles in solution (Njoki et al. 2007). The changes are best seen by UV–Vis spectroscopy, as shown in Fig. 5. Absorption spectra were recorded for aqueous dispersion of $Mo_6S_yI_z$ ($8.2 \leq y + z \leq 10$) nanowires before and after adding $HAuCl_4$ solution of different concentrations. Initially, the nanowire dispersion displayed strong absorption bands at around 290, 460, and 690 nm. After adding the lower-concentration solution, the spectrum is almost indistinguishable from the original spectrum. Only by adding five times 10 ml of the 0.25 mM solution, a broad and weak band centered at about 540 nm appears. The peak is more prominent if 10 ml of 2.5 mM chloroauric acid are introduced into the dispersion, which turns orange. By further adding chloroauric acid, the final dispersion becomes reddish with a very strong absorption band at 540 nm. These bands, which can be assigned to the plasmon band of gold nanoparticles, agree very well with the optical signatures of spherical gold nanoparticles in solution (Njoki et al. 2007). Njoki et al. have also shown that the wavelength of the surface-plasmon absorption band depends on the particle size and the maximum absorption wavelength λ_{max} increases with increasing diameter: from 519 nm for a diameter of around 20 nm to 569 nm for particles with a diameter of around 100 nm. The dependence can be described by a polynomial cubic curve $y = y_0 + ax + bx^2 + cx^3$ ($y_0 = 518.8$, $a = -0.0172$, $b = 0.0063$, and $c = -0.0000134$) yielding the average particle diameter in our samples of about 64 nm (for $\lambda_{max} = 540$ nm).

The average size of deposited gold nanoparticles was determined more accurately using microscopic methods. Figure 6a shows a SEM image of gold-decorated $Mo_6S_yI_z$ ($8.2 \leq y + z \leq 10$) nanowires (prepared with 2.5 mM $HAuCl_4$) dispersed in isopropyl alcohol and deposited on a silicon wafer. One clearly sees individual

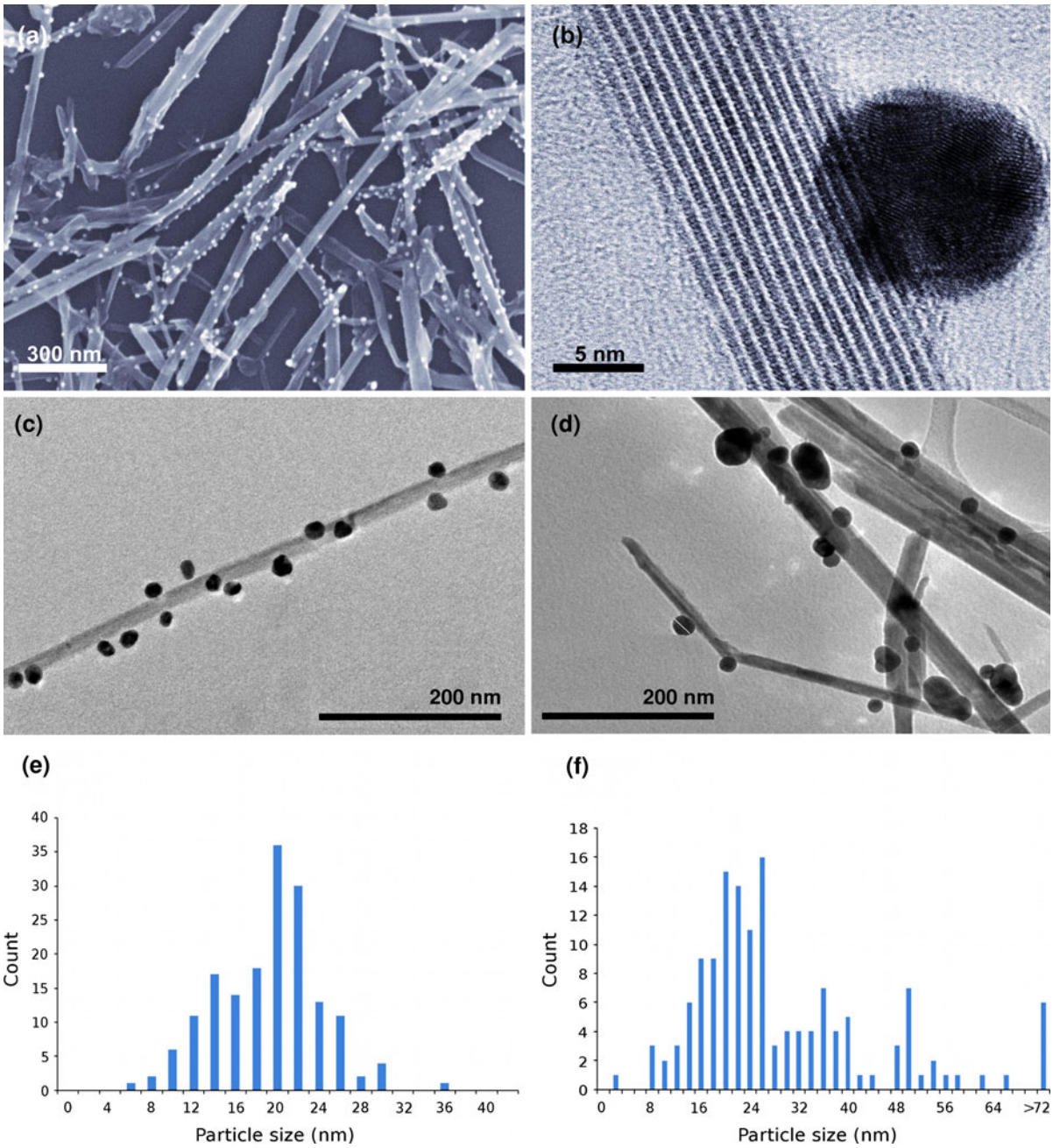

Fig. 6 SEM (**a**) and TEM (**b**) images of gold-decorated $Mo_6S_yI_z$ ($8.2 \leq y + z \leq 10$) nanowires. Several TEM images were recorded at low (**c**) and high (**d**) concentrations of $HAuCl_4$ in water. By zooming in, the diameters of the gold particles were measured. Analyzing over a hundred particles for each concentration, the histograms for lower (**e**) and higher (**f**) concentration were obtained. The average particle diameters are 19.2 and 23.3 nm, respectively

nanoparticles that are mostly spherical with diameters in the range of 10–65 nm. We find that by decreasing the concentration of $HAuCl_4$, the size of the gold nanoparticles remains almost unchanged, however, their number decreases significantly. At larger concentrations of chloroauric acid, some additional larger agglomerates are formed on the surface of nanowires.

A more precise size measurement was obtained from high-resolution TEM images (Fig. 6b). TEM images of decorated nanowires prepared with 0.25 and 2.5 mM

$HAuCl_4$ in water are shown in Fig. 6c and d, respectively. By zooming on each particle and obtaining images similar to Fig. 6b, we were able to measure the diameters of individual particles. Around 100 nanoparticles were randomly chosen from each sample and the obtained particle-size distributions are shown in Fig. 6e and f for 0.25 and 2.5 mM $HAuCl_4$ in water, respectively. The average diameter is found to be 19.2 nm for lower and 23.3 nm for higher concentration. Agglomerates with diameters larger than 72 nm, which represent around 3 % of all the particles, were excluded from the calculation of average diameters. We observe that the measured diameters differ significantly from the ones calculated from the UV–Vis spectra. However, one should note that in our case the nanoparticles interacted with and were attached to the nanowires instead of being in a water dispersion, and moreover, they were not monodisperse.

Sturdiness of deposition of gold nanoparticles on nanowires against ultrasonication has also been studied. Already during the decoration, the nanowire bundles were ultrasonicated to insure uniform distribution. We have verified and confirmed that the gold remained bound to the bundles even after 1 h of additional ultrasonication. The material is thus very stable and can be used in further experiments, dispersed in polar solvents (such as water, acetonitrile, isopropanol or ethanol). Also, we observed no difference in stabilities of the dispersions of nanowires and gold-decorated nanowires. Both remain stable for weeks in a 20 mg/1,000 ml dispersion without added surfactants.

In further experiments, a dispersion of purified nanowires was sprayed onto a silicon wafer using an airbrush spraying technique (Madaria et al. 2011). Keeping the nozzle-substrate separation at 5 cm, we were able to cover a surface of several cm^2 with nanowires. Shorter distances resulted in a non-uniform distribution of bundles and in formation of larger agglomerates as the air flow disturbed the sprayed solution before the solvent could evaporate. The uniformity of the deposition was improved by decreasing the concentration of nanowires in acetonitrile to around 1 mg/l and by decreasing the nozzle diameter. The latter, however, yielded a lower deposition rate. Using this technique, we were able to achieve a uniform deposition of almost isolated $Mo_6S_yI_z$ ($8.2 \leq y + z \leq 10$) bundles over the entire substrate with only small agglomerates. There was no apparent difference in the density of the nanowire bundles or in the formation of agglomerates between different regions of the sample. In the next step, silicon wafer with nanowire bundles was immersed in an aqueous solution containing $HAuCl_4$ and the obtained material is shown in Fig. 7. We noticed that while the bundles were decorated, the number of gold nanoparticles was significantly lower than on bundles decorated in dispersion at the same concentration of $HAuCl_4$ and at the same reaction time (see Fig. 6a). The density of nanoparticles on nanowires was further reduced if lower concentrations of chloroauric acid were used, however, the average diameter remained practically unchanged.

Instead of spraying the nanowires onto a silicon wafer, we also applied diluted dispersion of nanowires directly onto a copper mesh. The mesh was immersed into $HAuCl_4$ solution and a TEM image of a decorated bundle is shown in Fig. 8. Individual gold particles are visible on the bundle as well as larger aggregates, composed of individual nanoparticles. When comparing these decorated nanowires with the ones deposited onto silicon wafer under similar conditions (temperature, reaction time, concentration of $HAuCl_4$), we find the density of nanoparticles to be substantially higher. This is mainly because the bundles deposited on a substrate have a much smaller surface area accessible and because attachment to a substrate can influence the reactivity of the nanowires. One should

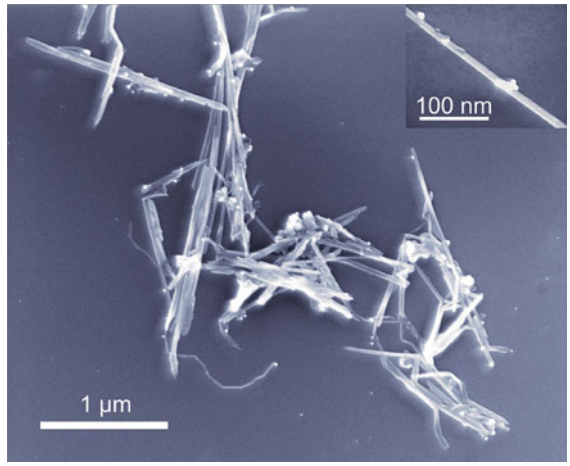

Fig. 7 SEM image of an agglomerate of $Mo_6S_yI_z$ ($8.2 \leq y + z \leq 10$) nanowires that were sprayed onto a silicon wafer, dipped into the 0.025 mM solution of chloroauric acid and left to dry. The close-up (inset) shows gold nanoparticles attached to the surface of nanowire bundles

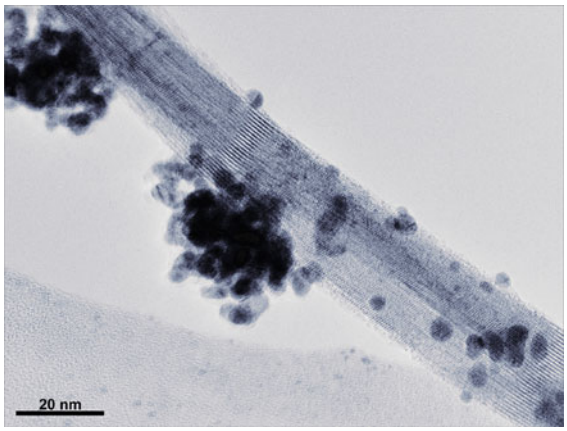

Fig. 8 TEM image of a nanowire bundle with gold nanoparticles. The nanowires were deposited directly to the Formvar/carbon coated copper mesh and dipped into a 0.025 mM solution of $HAuCl_4$. Individual gold nanoparticles are observed as well as larger agglomerates. Gold nanoparticles appear also on the surface of the copper grid as can be seen in the background in the *lower part* of the figure

note that while the densities of gold nanoparticles on nanowire bundles were higher if the decoration took place in a dispersion, the decoration of nanowires that have previously been deposited on a surface or on a grid has a much larger practical value for potential applications.

The underlying mechanism of nanowire decoration with gold nanoparticles can be understood by studying the reducing ability of $Mo_6S_yI_z$ ($8.2 \leq y + z \leq 10$) nanowires. We therefore performed cyclic voltammetry measurements and determined the oxidation and reduction potentials of the nanowires. We observed the reduction peak at $+0.71 \pm 0.07$ V and the oxidation peak at -0.83 ± 0.05 V relative to the standard hydrogen electrode. Taking into account that the reduction potential for $[AuCl_4]^-$ in aqueous solution is 1.002 V (CRC Handbook 2001), we propose the following redox reaction for the decoration process, where $Mo_6S_yI_z$ ($8.2 \leq y + z \leq 10$) nanowires are abbreviated as MoSI (NW):

$$[AuCl_4]^- + 3\text{MoSI (NW)} \rightarrow \text{Au}^0 + 3\text{MoSI(NW)}^+ + 4Cl^-.$$

Since the surface layers of nanowire bundles are composed of iodine and sulfur atoms, the nanowires themselves serve as capping agent stabilizing the gold nanoparticles after the reduction of $[AuCl_4]^-$.

While we believe that the redox reaction is the main mechanism for the stable decoration of the nanowires, dangling bonds at the ends of individual nanowires can also contribute to the successful decoration with gold nanoparticles. Unlike other crystalline nanowires, these molecular nanowires are namely composed of repeating molecular units, consisting of clusters, which are joined together by sulfur bridges (Nicolosi et al. 2007). Individual wires terminate with sulfur atoms and since the nanowires are of different lengths and shifted relative to each other, there exist many dangling bonds forming additional reaction sites capable of reducing $[AuCl_4]^-$.

Transformation of decorated $Mo_6S_yI_z$ ($8.2 \leq y + z \leq 10$) nanowires to decorated MoS_2 nanotubes

We have shown previously that $Mo_6S_yI_z$ ($8.2 \leq y + z \leq 10$) nanowires can be used as precursors for production of MoS_2 multi-wall nanotubes (Remškar et al. 2009). It has later been shown that sulfurization of thinner bundles (diameters of around 100 nm) synthesized at chemical transport reaction conditions also leads to formation of MoS_2 nanotubes (Remškar et al. 2011). The obtained nanotubes preserved the hedgehog-like shape of the precursor nanowires.

Using gold-decorated nanowires as precursors, we performed sulfurization under the same conditions as Remškar et al. to see if gold nanoparticles remained attached during the reaction. The obtained material is shown in Fig. 9, showing SEM and TEM images of the multi-wall MoS_2 nanotubes decorated with gold nanoparticles. The diameters of the nanotubes, which retained the shape of the precursor bundles, were typically between 20 and 40 nm at a wall thickness of 5-10 nm. Although the walls often showed imperfections, the (002) planes running parallel to the tube growth were easily identifiable. From a close-up of the edge of the nanotube (Fig. 9b inset), the spacing between the planes was measured and found to be 0.62 nm, which is in excellent agreement with the data found in the literature (Therese et al. 2006). While the majority of gold nanoparticles remained well preserved during the sulfurization, we observed some particles attached to the nanotubes that were significantly larger than the average ones. Their appearance can be explained by partial coalescence of the attached nanoparticles.

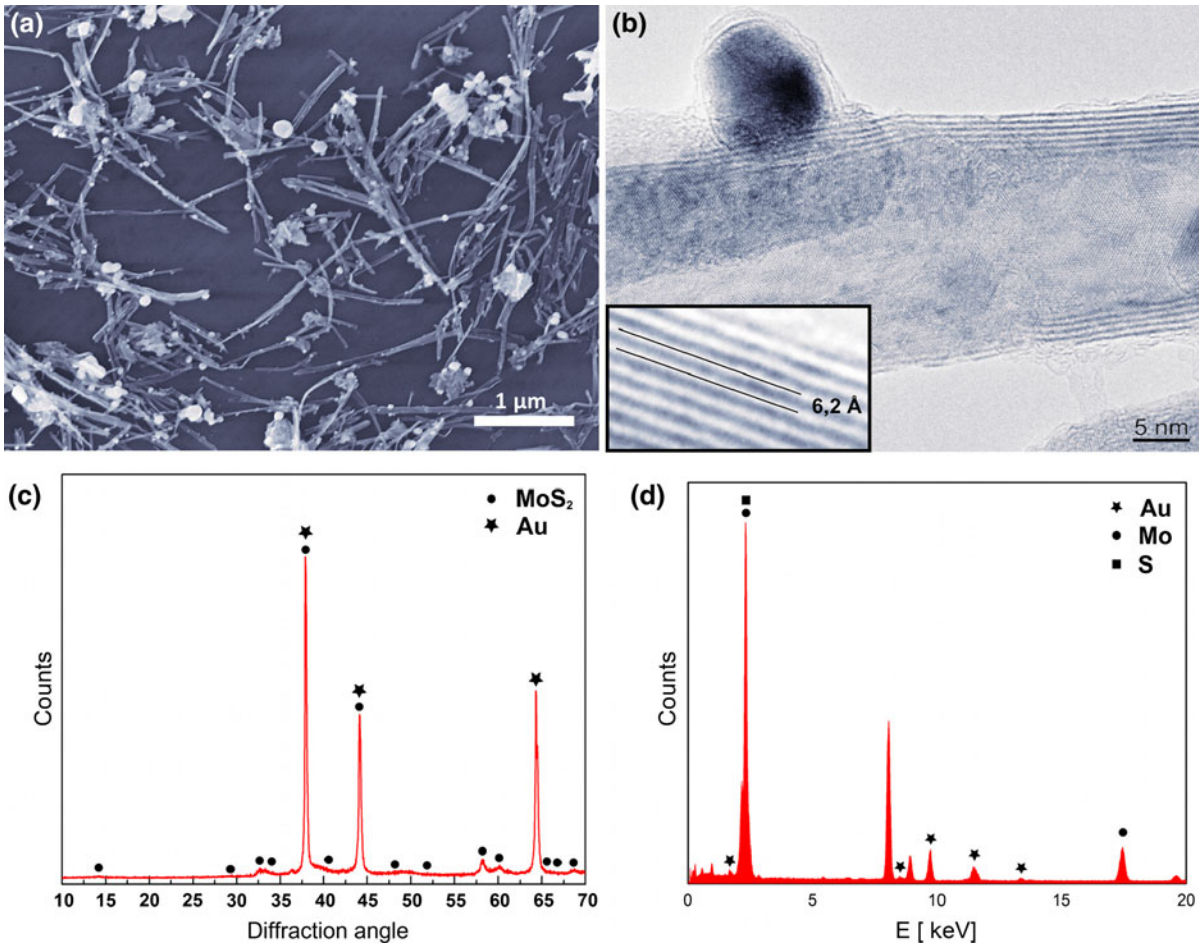

Fig. 9 Decorated nanowires were transformed into decorated MoS_2 nanotubes. SEM (**a**) and TEM (**b**) images of decorated nanotubes. Inset shows a close-up on the wall of the tube that was used to determine the interlayer spacing. XRD (**c**) and EDS (**d**) confirmed that the transformation from nanowires to nanotubes was complete as only decorated MoS_2 nanotubes were observed

The products were further analyzed by X-ray powder diffraction (Fig. 9c). The majority of the peaks in the spectrum can be assigned to MoS_2 nanotubes (according to JCPDS-No. 77-1716); however, three intense peaks corresponding to the (111), (200), and (220) Bragg reflections on gold nanocrystals were also observed. In addition, EDS was performed on the synthesized material (Fig. 9d) to prove that iodine was completely removed during the sulfurization process with only molybdenum, sulfur and gold showing in the spectrum. This confirms that pure MoS_2 nanotubes decorated with gold nanoparticles were obtained.

We have also verified and confirmed that gold nanoparticles remained bound to the MoS_2 nanotubes even after 1 h of additional ultrasonication, similar as the original $Mo_6S_yI_z$ ($8.2 \leq y + z \leq 10$) nanowires.

Conclusions

We presented a simple yet efficient method for synthesis and purification of bundles of thin $Mo_6S_yI_z$ ($8.2 \leq y + z \leq 10$) nanowires. The synthesized nanowires were much thinner than obtained by other methods (40 nm in comparison to a hundred or several hundred nm) and were in contrast fully dispersible in water without added surfactants, which is crucial for homogeneous decoration. The nanowire dispersion remains stable for at least several weeks. This facile and efficient process enables

production of several hundred milligrams of nanowire bundles at a time, which makes the material and the described procedure even more attractive for possible industrial applications.

The decoration was done in a simple and convenient wet-chemical method that enables efficient self-decoration of nanowires with gold nanoparticles at room temperature without any additional reducing reagents. We were able to successfully decorate nanowires with gold both in the solution and on a substrate and have shown that the decorated nanowires form a stable dispersion in polar solvents. The described procedure is one of the few examples of redox templating at room temperature without use of reducing agent to produce metal-decorated nanowires.

In addition, we have shown that using gold-decorated nanowires as precursor material, gold-decorated MoS_2 nanotubes dispersible in different polar solvents can be obtained. By reducing the diameters of the nanowires, we were able to obtain very thin gold-decorated nanotubes. The presented method facilitates functionalization of otherwise biologically and chemically inert nanotubes and opens new perspectives for fabrication of different nanodevices, including biological nanosensors.

Acknowledgments The authors thank Jan Ravnik for performing the cyclic voltammetry measurements. We also acknowledge the support of Slovenian Research Agency (P1-0192, P1-0040).

References

Burda C, Chen XB, Narayanan R, El-Sayed MA (2005) Chemistry and properties of nanocrystals of different shapes. Chem Rev 105:1025–1102

CRC handbook of chemistry and physics 82nd edn. CRC Press, Boca Raton (2001)

Compagnini G, Patanè G, Sinatra M, Puglisi O, Nicolosi V, Mihailović D, Vengust D, Strle J (2010) Bonding states in molecular-scale MoSI nanowire-gold nanoparticle networks. J Phys Chem Lett 1:393–397

Daniel MC, Astruc D (2004) Gold nanoparticles: assembly, supramolecular chemistry, quantum-size-related properties, and applications toward biology, catalysis, and nanotechnology. Chem Rev 104:293–346

Domenici V, Conradi M, Remškar M, Viršek M, Zupančič B, Mrzel A, Chambers M, Zalar B (2011) New composite films based on MoO_{3-x} nanowires aligned in a liquid single crystal elastomer matrix. J Mater Sci 46:3639–3645

Gadermaier C, Kušar P, Vengust D, Vilfan I, Mihailović D (2007) Equilibrium and non-equilibrium optical properties of MoSI nanowires. Phys Status Solidi B 244:4152–4156

Hernández-Vélez M (2006) Nanowires and 1D arrays fabrication: an overview. Thin Solid Films 495:51–63

Homola J (2008) Surface plasmon resonance sensors for detection of chemical and biological species. Chem Rev 108:462–493

Joshi RK, Hu Q, Alvi F, Joshi N, Kumar A (2009) Au decorated zinc oxide nanowires for CO sensing. J Phys Chem C 113:16199–16202

Kovič A, Žnidaršič A, Jesih A, Mrzel A, Gaberšček M, Hassanien A (2012) A novel facile synthesis and characterisation of molybdenum nanowires. Nanoscale Res Lett 7:567

Lee SH, Sung JH, Park TH (2012) Nanomaterial-based biosensor as an emerging tool for biomedical applications. Ann Biomed Eng 40:1384–1397

Madaria AR, Kumar A, Zhou C (2011) Large scale, highly conductive and patterned transparent films of silver nanowires on arbitrary substrates and their application in touch screens. Nanotechnology 22:245201

Meden A, Kodre A, Padežnik Gomilšek J, Arčon I, Vilfan I, Vrbanič D, Mrzel A, Mihailović D (2005) Atomic and electronic structure of $Mo_6S_{9-x}I_x$ nanowires. Nanotechnology 16:1578–1583

Nicolosi V, Nellist PD, Sanvito S, Cosgriff EC, Krishnamurthy S, Blau WJ, Green LH, Vengust D, Dvoršek D, Mihailović D, Compagnini G, Sloan J, Stolojan V, Carey JD, Pennycook SJ, Coleman JN (2007) Observation of van der Waals driven self-assembly of MoSI nanowires into a low-symmetry structure using aberration-corrected electron microscopy. Adv Mater 19:543

Njoki PN, Lim IIS, Mott D, Park HY, Khan B, Mishra S, Sujakumar R, Luo J, Zhong CJ (2007) Size correlation of optical and spectroscopic properties for gold nanoparticles. J Phys Chem C 111:14664–14669

Ploscaru MI, Kokalj SJ, Uplaznik M, Vengust D, Turk D, Mrzel A, Mihailović D (2007) $Mo_6S_{9-x}I_x$ nanowire recognitive molecular-scale connectivity. Nano Lett 7:1445–1448

Ramgir NS, Yang Y, Zacharias M (2010) Nanowire-based sensors. Small 6:1705–1722

Rangus M, Remškar M, Mrzel A (2008) Preparation of vertically aligned bundles of $Mo_6S_{9-x}I_x$, $(4.5 < x < 6)$ nanowires. Microelectron J 39:475–477

Remškar M, Viršek M, Mrzel A (2009) The MoS_2 nanotube hybrids. Appl Phys Lett 95:133122

Remškar M, Mrzel A, Viršek M, Godec M, Krause M, Kolitsch A, Singh A, Seabaugh A (2011) The MoS_2 nanotubes with defect-controlled electric properties. Nanoscale Res Lett 6:26

Singh N, Gupta RK, Lee PS (2011) Gold-nanoparticle-functionalized In_2O_3 nanowires as CO gas sensors with a significant enhancement in response. ACS Appl Mater Interfaces 3:2246–2252

Syed MA, Bokhari SHA (2011) Gold nanoparticle based microbial detection and identification. J Biomed Nanotechnol 7:229–237

Tahir MN, Zink N, Eberhardt M, Therese HA, Kolb U, Theato P, Tremel W (2006) Overcoming the insolubility of molybdenum disulfide nanoparticles through a high degree of sidewall functionalization using polymeric chelating ligands. Angew Chem Int Ed 45:4809–4815

Therese HA, Zink N, Kolb U, Tremel W (2006) Synthesis of MoO_3 nanostructures and their facile conversion to MoS_2 fullerenes and nanotubes. Solid State Sci 8:1133–1137

Vrbanič D, Remškar M, Jesih A, Mrzel A, Umek P, Ponikvar M, Jančar B, Meden A, Novosel B, Pejovnik S, Venturini P, Coleman JC, Mihailović D (2004) Air-stable monodispersed $Mo_6S_3I_6$ nanowires. Nanotechnology 15:635–638

Vrbanič D, Pejovnik S, Mihailović D, Kutnjak Z (2007) Electrical conductivity of $Mo_6S_3I_6$ and $Mo_6S_{4.5}I_{4.5}$ nanowires. J Eur Ceram Soc 27:975–978

Wanekaya AK, Chen W, Myung NV, Mulchandani A (2006) Nanowire-based electrochemical biosensors. Electroanalysis 18:533–550

Xia YN, Halas NJ (2005) Shape-controlled synthesis and surface plasmonic properties of metallic nanostructures. MRS Bull 30:338–348

Yogeswaran U, Chen SM (2008) A review on the electrochemical sensors and biosensors composed of nanowires as sensing material. Sensors 8:290–313

Zhang R, Hummelgård M, Dvoršek D, Mihailović D, Olin H (2010) $Mo_6S_3I_6$–Au composites: synthesis, conductance, and applications. J Colloid Interface Sci 348:299–302